# RECENT ADVANCES IN SOLID POLYMER ELECTROLYTE FUEL CELL TECHNOLOGY WITH LOW PLATINUM LOADING ELECTRODES

SUPRAMANIAM SRINIVASAN*, DAVID J. MANKO, HERMANN KOCH†, MOHAMMAD A. ENAYETULLAH and A. JOHN APPLEBY

*Center for Electrochemical Systems and Hydrogen Research, Texas Engineering Experiment Station, Texas A&M University System, College Station, TX 77843-3577 (U.S.A.)*

## Summary

Of all the fuel cell systems, only alkaline and solid polymer electrolyte fuel cells are capable of achieving high power densities (>1 W $cm^{-2}$) required for terrestrial and extraterrestrial applications. Electrode kinetic criteria for attaining such high power densities are discussed. Attainment of high power densities in solid polymer electrolyte fuel cells has been demonstrated earlier by different groups using high platinum loading electrodes (4 mg $cm^{-2}$). Recent work at Los Alamos National Laboratory and at Texas A&M University (TAMU) demonstrated similar performance for solid polymer electrolyte fuel cells with ten times lower platinum loading (0.45 mg $cm^{-2}$) in the electrodes. Some of the results obtained at TAMU are discussed in terms of the effects of type and thickness of membrane, and of the methods of platinum localization in the electrodes, on the performance of a single cell.

## 1. Introduction

### *1.1. Rationale for selection of solid polymer electrolyte instead of alkaline electrolyte fuel cell system for attainment of high power densities*

Only the alkaline and solid polymer electrolyte fuel cell systems are capable of attaining high power densities (>1 W $cm^{-2}$). The pros and cons of the two fuel cell systems are best expressed in Table 1. Even though the alkaline fuel cell systems developed by International Fuel Cells/United Technologies Corporation [1] for the Apollo and Space Shuttle Program are in a highly advanced state, and have functioned extremely well for the required missions, the solid polymer electrolyte fuel cell system is a stiff competitor for the alkaline fuel cell system, as is clearly evident in Table 1. There is already a sufficient Technology Base Development for the alkaline

*Author to whom correspondence should be addressed.
†Exchange Graduate Student from Ruhr University, Bochum, F.R.G.

0378-7753/90/$3.50 

TABLE 1

Pros and cons of solid polymer electrolyte fuel cell system over alkaline electrolyte fuel cell system for (WPAFB'S) proposed application of high power density electric generation systems

| Solid polymer electrolyte fuel cell system | Alkaline fuel cell system |
|---|---|
| *Pros* | *Pros* |
| 1. Electrolyte is a perfluorinated sulfonic acid membrane–only water need be added to make it conducting | 1. The only well developed fuel cell system (kW level) for space application. |
| 2. Excellent electrode kinetics of hydrogen oxidation in this electrolyte — overpotential at 2 A $cm^{-2}$ is only 20 mV. | 2. Best electrode kinetics of oxygen reduction at temperatures less than 200 °C — low Tafel slope. |
| 3. Electrode kinetics of oxygen reduction faster in this electrolyte than in any other acid electrolytes. | 3. High conductivity of the electrolyte. |
| 4. Membrane has a high bubble pressure (even at thickness of order of 50 $\mu$m) and is, hence, a good gas separator. | 4. By operation at over 100 °C, water removal is simplified. |
| 5. High power density attained approaching same level as in alkaline electrolyte fuel cell. | |
| *Cons* | *Cons* |
| 1. High cost of membrane. | 1. Highly corrosive environment. |
| 2. A more complex but manageable water management problem. | 2. Electrolyte has to be held in matrix to reduce ohmic drops. |
| 3. Insufficient data on stability of materials in SPE® membranes, particularly at elevated temperatures. | 3. Difficult to find matrix with required bubble pressure. |
| | 4. Electrolyte has to be replenished in matrix via electrolyte reservoir plate behind electrode. |
| | 5. Leak-proof seals in cells difficult. |
| | 6. Electrolyte degrades electrode structure. |
| | 7. Electrode kinetics of hydrogen oxidation considerably slower in alkaline than in solid polymer electrolyte. |

system at International Fuel Cells/United Technologies Corporation and several $100 M have been invested in this system. Even though a considerably lesser financial support has been provided for the solid polymer electrolyte system, it is in an advanced state of development, as evidenced by the progress made in the development of 1.5 kW systems by Ballard Technologies, Inc. in Vancouver, Canada [2] and by Ergenics Power Systems, Inc., in Wyckoff, New Jersey [3]. Siemens [4] in Erlangen, Germany, is also engaged in research, development and demonstration of high power density solid polymer electrolyte fuel cell systems for submarine applications. The work on solid polymer electrolyte fuel cell systems by these organizations has been with high platinum loading (4 mg $cm^{-2}$) electrodes. In the most recent work at Ballard, it has been reported that a current density ($i$) of 6 A $cm^{-2}$ has been attained at cell potential ($E$) of 0.5 V. The slope of the linear region in Ballard's $E$–$i$ plot is 0.08 ohm $cm^2$. The performance of relatively high power densities (1 A $cm^{-2}$ at 0.7 V) in solid polymer electrolyte fuel cells with low platinum loading electrodes was first demonstrated at Los Alamos National Laboratory by Srinivasan *et al.* [5 - 7].

The solid polymer electrolyte fuel cell system has major advantages over the alkaline fuel cell system in terms of lower operating temperature, ability to start from cold, and total lack of electrolyte management problems. From a cold (10 °C) start-up, this system can be designed to give full power in under 30 s. The fuel cell system can easily be programmed for instant start-up by arranging a stack hydrogen dead-volume, after the cut-off valve, equal to twice the corresponding oxygen cut-off-dead-volume. Short-circuiting will rapidly reduce hydrogen and oxygen partial pressures to close to zero, with production of water that is sealed into the stack, and so will maintain the membrane in peak condition. Thus, a cold, solid polymer electrolyte fuel cell stack can be safely and indefinitely left on open circuit, if prevented from freezing, and it can still be ready for rapid start-up. This is a great advantage compared with the high-performance alkaline fuel cell system, which must be maintained at the required minimum temperature to prevent electrolyte solidification, and whose open-circuit storage under these conditions is doubtful.

### *1.2. Necessary electrode kinetic criteria for attainment of high power densities*

The heart of the fuel cell system is the electrochemical cell. Even though the electrode kinetics of the electrochemical cell have been adequately dealt with in books [8, 9] and review articles in journals [10], it is worth recapitulating the electrode kinetic criteria for attainment of high power densities. As will be seen from the brief analysis presented below, the electrode kinetics of fuel cell reactions pose the critical issues and problems.

First, there is no doubt that the only fuel cells which are capable of attaining high power densities are the ones using hydrogen and oxygen as reactants. Second, it has been clearly demonstrated that only the fuel cells with alkaline and perfluorinated sulfonic acid polymer electrolytes are

capable of attaining high power densities. The main reason for this is that there is hardly any anion adsorption on electrocatalysts from these electrolytes and thus the poisoning of the oxygen reduction reaction is minimal. Third, in fuel cells with both these electrolytes, mass transport limitations are not visible at current densities up to several A $cm^{-2}$. Under these conditions, the cell potential ($E$)–current ($i$) relations may be expressed by the equation:

$$E = E_0 - b \log i - Ri \tag{1}$$

In perfluorinated sulfonic acids and their polymeric acids (*e.g.*, Nafion®*), the kinetics of hydrogen oxidation is extremely fast and the potential of the hydrogen electrode varies linearly with current density up to high current densities (a few A $cm^{-2}$) [7]. In alkaline electrolytes, this is not the case because the exchange current density for this reaction is considerably less than in the perfluorinated sulfonic acids [11]. However, the oxygen reduction reaction is faster in alkaline medium than in perfluorinated sulfonic acids. In both media, the relation between the oxygen electrode potential and current density is semi-logarithmic, and this accounts for the second term in the right hand side of eqn. (1). In this equation, $b$ represents the Tafel slope for the oxygen reduction reaction. The first term on the right hand side may be further expressed by:

$$E_0 = E_r - b \log i_0 \tag{2}$$

where $E_r$ is the reversible potential for the cell and $i_0$ is the exchange current density for the oxygen reduction reaction. Differentiating eqn. (1), one obtains:

$$\frac{dE}{di} = -\frac{b}{i} - R \tag{3}$$

At low current densities, the first term on the right hand side of eqn. (3) is predominant and is reflected in the high slope (which gradually decreases) of the cell potential–current density plot (see Fig. 1). At higher current densities, the second term becomes important and is responsible for the linear region in this plot. Contributions to $R$ are from:

(i) the ionic resistance of the electrolyte;

(ii) electronic resistance of the electrodes;

(iii) charge transfer resistance of the hydrogen electrode;

(iv) charge transfer resistance of the oxygen electrode which is due to the difference in the activation overpotential between the two current densities over which the slope was measured;

(v) any small contributions to mass transport resistances.

As will be seen from Fig. 1, if mass transport becomes important there will be a rapid fall-off of cell potential with current density and, thus, only close to the limiting current density does mass transport control exert its influence. This apparently simplified equation applies over 3 decades of

*Nafion®, E.I. DuPont Trademark.

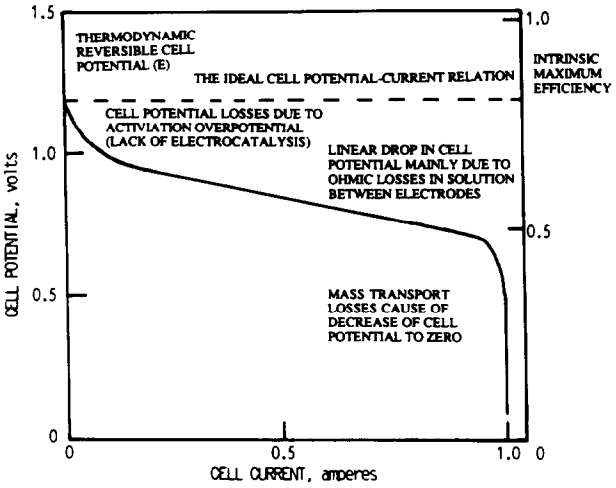


Fig. 1. Typical plot of cell potential *vs.* current for fuel cells, illustrating regions of control by various types of overpotentials.

current density (1 mA $cm^{-2}$ - 2 A $cm^{-2}$) for high power density solid polymer electrolyte fuel cells (see Section 3).

It is worthwhile at this stage to focus on the electrode kinetic requirements to attain high power densities by an examination of eqns. (1) - (3) and Fig. 1. Two factors clearly dominate the shape of the cell potential–current density relation: these are the Tafel parameters for the oxygen reduction reaction and the ohmic overpotential in the cell. The highest values of the exchange current density for oxygen reduction in porous gas diffusion electrodes is approximately $10^{-6}$ A $cm^{-2}$. The minimum value of $R$ in eqn. (1) which has been reported is 0.05 Ω $cm^2$ for the alkaline fuel cell system (operating at 150 °C and 8 atm) and 0.08 Ω $cm^2$ for the solid polymer electrolyte fuel cell system (operating at 95 °C and 5 atm). In alkaline electrolytes, the Tafel slope for oxygen reduction on the best electrocatalyst (90% Au, 10% Pt) is 0.04 V/decade, whereas in solid polymer electrolytes it is 0.06 V/decade. The best reported cell performance in the alkaline fuel cell system is at a temperature of 150 °C and 8 - 10 atm pressure. In the solid polymer electrolyte fuel cell system, most of the work has been carried out at close to 100 °C, whereas the best reported performance by Ballard Technologies, Inc. is at 120 °C. Use of a value of $E_r$ = 1.20 V is a close approximation for the reversible potential of the fuel cell in both these environments. Thus, at a current density of 3 A $cm^{-2}$, and a cell potential of 0.8 V (an expected performance of fuel cells for defense applications), one may write the following expressions for the exchange current densities of the oxygen reduction reaction:

Alkaline fuel cell:

$$0.8 = 1.20 + 0.04 \log i_0 - 0.04 \log 3 - 0.05 \times 3 \quad (4)$$

$$\therefore i_0 = 1.7 \times 10^{-6} \text{ A cm}^{-2}$$

SPE fuel cell:

$$0.8 = 1.20 + 0.06 \log i_0 - 0.06 \log 3 - 0.10 \times 3 \quad (5)$$

$$\therefore i_0 = 6.5 \times 10^{-2} \text{ A cm}^{-2}$$

This simplified analysis signifies that the exchange current density for oxygen reduction in alkaline electrolyte must be equal to, or greater than, about $2 \times 10^{-6}$ A $cm^{-2}$ (based on the geometric area of the electrode) to reach the specified goals. On the other hand, with the value of $R$ (0.1 $\Omega$ $cm^2$) assumed for the solid polymer electrolyte, the exchange current density for the oxygen reduction reaction will have to be greater than $7 \times 10^{-2}$ A $cm^{-2}$ (again based on the geometric area of the electrode). If, however, we were to assume the same value of $R$ for the solid polymer electrolyte fuel cell as that for the alkaline fuel cell, the exchange current density for the oxygen reduction will have to be $2 \times 10^{-4}$ A $cm^{-2}$. Considering the exchange current densities, which have been reported for oxygen reduction on smooth surfaces in alkaline ($i_0 = 10^{-8}$ A $cm^{-2}$) and fluorinated sulfonic acid ($i_0 = 10^{-7}$ A $cm^{-2}$) electrolytes at room temperature, and assuming (i) an increase of these values by a factor of 10 for operation at elevated temperatures (150 °C for the alkaline fuel cell system and 120 °C for the SPE fuel cell system), and (ii) a conservative value of 100 for the roughness factor of the porous electrodes, it should be possible to reach the desired goal of operation at 3 A $cm^{-2}$ and 0.8 V/cell only if the slope of the linear region of the cell potential–current density is 0.05 $\Omega$ $cm^2$ or less.

### *1.3. A snapshot version of the status of solid polymer electrolyte fuel cell technology*

In three recent articles [5 - 7] the present status of the solid polymer electrolyte fuel cell technology is summarized. For detailed information, the reader is referred to these publications. In this paper a "snapshot" version (Table 2) of the progress made in this field is presented. Table 2 demonstrates that significant progress has been made during the 1980s in solid polymer electrolyte fuel cell technology, in spite of the fact that the funding for this program is miniscule compared with the investments made for the development of alkaline, phosphoric, molten carbonate, and solid oxide fuel cells. In hardware production of solid polymer electrolyte fuel cells, Ballard Technologies Corporation and Ergenics Power Systems, Inc. have done extremely well. Both are at a stage where they can custom-make 1.5 kW power plants. However, these systems, as well as those previously developed by General Electric Company, contain electrodes with high platinum loadings (4 mg $cm^{-2}$). The first demonstration of high power density, solid polymer electrolyte fuel cells, with low platinum loading electrodes was by one of the present authors (SS) and his coworkers at Los Alamos National Laboratory (LANL); a brief description of this work is presented in the next subsection.

TABLE 2

A snapshot version of the progress made in solid polymer electrolyte fuel cell technology

| Organization (period of activity) | Performance | Major accomplishments | Major problems |
|---|---|---|---|
| 1. General Electric/Hamilton Standards-UTC (1958 - present) | Gemini Fuel Cells — 1 kW, 30 kg, 100 mA $cm^{-2}$ at 0.5 V; Significant improvement in performance when Nafion instead of polystyrene sulfonate used as electrolyte. | First major application of fuel cells; breakthrough by utilizing perfluorinated sulfonic acid electrolyte membrane. | Pt-loading (4 mg $cm^{-2}$); difficult water management; mass transport limitations at lower current densities than expected with $H_2$/Air |
| 2. Ballard Technologies Corporation, Vancouver, Canada (1980 -) | Best performance: 6 A $cm^{-2}$ at 0.5 V with $H_2/O_2$; slope of $E$–$i$ plot linear region 0.08 $\Omega$ $cm^2$; with $H_2$/air 2 A $cm^{-2}$ at 0.55 V. | 1.5 kW units built and tested; use of Dow membranes instead of Nafion significantly improves performance | Pt loading high (4 mg $cm^{-2}$); lifetime not known. |
| 3. Siemens, Erlangen Germany (1986 -) | Technology similar to General Electric/ Hamilton Standards-UTC; high power densities, same as Ballard, reported. | Demonstration of high power densities | |
| 4. Ergenics Power Systems, Inc. (1984 -) | 200 W units with hydride storage, built and tested — for power required by astronauts in spacewalks; best performance reported 400 mA $cm^{-2}$ at 0.7 V. | Novel approach for water management — internal transport of water from porous carbon behind electrode for humidification of gases and membrane; 1.5 kW units custom-made. | High Pt loading (4 mg $cm^{-2}$); performance on $H_2/O_2$ is good; with $H_2$/Air, mass transport limitations at current densities less than expected. |
| 5. Los Alamos National Laboratory (1981 -) | 2 A $cm^{-2}$ at 0.5 V attained in 5 $cm^2$ cells with $H_2/O_2$ as reactants; 50 $cm^2$ cells designed and tested; Dow membrane gives best performance. | Low Pt loading electrodes (0.4 mg $cm^{-2}$); localization of Pt near front surface of electrode to attain high power density; optimization of humidification conditions of cell; theoretically expected performance with air at current densities up to 1 A $cm^{-2}$. | Program too electrochemical research oriented; needs emphasis on engineering aspects — thermal and water management. |
| 6. Texas A&M University (1987 -) | 2 A $cm^{-2}$ at 0.6 V attained with $H_2/O_2$ as reactants in 5 $cm^2$ cell; at same current density cell potential 0.38 V with 50 $cm^2$ cell; design improved; Dow membrane gives best performance. | Alternative and more economical methods for Pt localization being developed; thermal and water management investigations initiated. | Performance improvement necessary in low current density region to reach WPAFBs goals of 3 A $cm^{-2}$ at 0.8 V. |

*1.4. A synopsis of advances in the attainment of high power densities in solid polymer electrolyte fuel cells with low-platinum-loading electrodes*

Since the first Space Electrochemical Research and Technology (SERT) Conference, in which the results of the first set of investigations on solid polymer electrolyte fuel cells with low-platinum-loading electrodes were presented [5], there has been considerable progress in developing methods for the attainment of high power densities (about 0.7 W $cm^{-2}$) in such types of fuel cells. It must be noted that the Nafion membrane was used as the proton-conducting membrane in all these investigations. The methods used to attain the high power densities may be summarized as follows:

(i) optimization of the amount of Nafion impregnated into the electrode structure;

(ii) hot-pressing of the Nafion-impregnated electrodes to prepurified Nafion membranes at 120 °C (close to glass transition temperature) and 50 atm pressure;

(iii) optimization of the humidification of the reactant gases at a temperature of 5 °C for oxygen or air, and 10 - 15 °C for hydrogen, above the cell temperature;

(iv) operation of the cell at elevated temperatures and pressures (say, 80 °C and 5 atm);

(v) localization of platinum by fabrication of electrodes with a higher percentage of platinum crystallites on high surface area carbon (*i.e.*, supported electrocatalysts with 20 wt.% Pt/C rather than 10%) while still maintaining the amount of Pt in the electrode (0.4 mg $cm^{-2}$), and by sputter-deposition of a thin film of platinum on the front surface (0.05 mg $cm^{-2}$), corresponding to a 500 Å film on a smooth surface).

By use of all these methods, it was possible to attain a current density of 1 A $cm^{-2}$ at a cell potential of 0.64 V with $H_2/O_2$ as reactants, and 0.580 V with $H_2$/air reactants at 80 °C and 3/5 atm pressure (3 on hydrogen and 5 on oxygen side).

The cell potential ($E$)–current density ($i$) plot fitted eqn. (1). The electrode kinetic parameters for the cell, $E_0$, $b$, and $R$, were calculated using a non-linear least squares fit of this equation to the experimental points. The slope of the Tafel line for oxygen reduction was found to be 0.050 - 0.060 V/decade and was independent of temperature.

Since small variations in the parameter $b$ give rise to misleading values of $i_0$, it was decided to use the current density at a cell potential of 0.900 mV (at this potential mass transport and ohmic effects are negligible, and so also is the overpotential at the hydrogen electrode) as a measure of the electrocatalytic activity of the electrode for the oxygen reduction reaction. It is extremely important to have this value as high as possible to minimize the steep decrease of slope of the cell potential–current density region at very low values of current densities. In the best case, *i.e.*, with $H_2/O_2$ as reactants at 3/5 atm and 80 °C, in cells with electrodes composed of 20% Pt/C supported electrocatalysts and 0.4 mg Pt $cm^{-2}$ on to which a thin film of Pt was sputtered, the current density at 0.900 V was 160 mA $cm^{-2}$.

Further, the calculated value of $R$ (0.24 $\Omega$ cm$^2$) was quite close to the high frequency resistance (0.21 $\Omega$ cm$^2$), indicating the absence of mass transport overpotential over the measured current density range. The increase of cell potential with pressure, at constant current density, showed the expected semi-logarithmic dependence. The cyclic voltammetric technique was used to determine the electrochemically active surface area of the electrode. By use of this method, the platinum utilization of the electrode, with the best configuration of electrodes (20% Pt/C 0.40 mg Pt cm$^{-2}$) plus sputtered film (0.05 mg Pt cm$^{-2}$), was found to be about 15 - 20%. It was concluded in the second publication [7] since the SERT conference that to increase the power densities further, it is necessary to use membranes with higher specific conductivities and better water retention characteristics.

*1.5. Scope of present work*

The work described in the preceding subsection was carried out by one of the authors (SS) of this paper and his former colleagues at LANL. This work has since then been continued in our laboratories with the objective of increasing the power densities still further, as required for some applications (for example, silent mobile power source for transportation). While the work at LANL was focussed on developing solid polymer electrolyte fuel cells using reformed hydrogen (steam-reforming of methanol), the work at our Center (CESHR) is concentrating on developing fuel cells using pure $H_2$ and $O_2$. As seen from the results in the preceding section, the "high priority" tasks which are envisioned to be important are: (i) to develop methods, alternative to sputter-deposition, to localize platinum near the front surface of the electrode; (ii) to reduce the ohmic overpotential in the cell. The reason for the importance of the former is that sputter-deposition is not economically feasible compared with wet-chemical methods, which can be automated, for the large-scale modification of surfaces of electrodes for fuel cell systems with a reasonable power output (20 kW and higher). The methods, which are examined in this work for the deposition of a thin layer of Pt on the front surface of the electrodes are:

(i) brushing the surface with a chloroplatinic acid solution (desired quantity and drying);

(ii) brushing the surface with platinum black particles suspended in Nafion solution;

(iii) electrodeposition of Pt.

Two approaches were taken to reduce the ohmic overpotential in the cell: use of (i) thinner membranes; (ii) Dow membranes with better conductivity and water retention characteristics.

## 2. Experimental

### *2.1. Wet chemical/electrochemical methods to localize platinum near front surfaces*

The membrane and electrode (M&E) assemblies were fabricated using Protech porous gas diffusion electrodes (20% Pt/C, 0.4 mg $cm^{-2}$) and proton conducting polymer membranes (Dupont and Dow Chemical). Localization of an extra layer of platinum on the active surface of these electrodes was achieved by wet chemical methods:

(i) brushing with Nafion solution containing unsupported Pt catalyst;

(ii) chemical deposition of Pt from $H_2PtCl_6$;

(iii) electrochemical deposition of Pt, also from $H_2PtCl_6$.

In the first method, 0.5 mg of fuel cell grade unsupported Pt catalyst (Prototech) was sonicated in 5% Nafion solution (0.6 ml), and two electrodes (each of 5 $cm^2$ area) were brushed with the mixture, using a soft printing brush, as uniformly as possible. The brushed electrodes were next dried in a vacuum oven at 70 °C and then impregnated with Nafion, in the manner described in previous publications [5 - 7], prior to fabrication of the M&E assembly. Chemical deposition of Pt (0.5 mg $cm^{-2}$) was carried out by brushing the active surface of the electrodes with an appropriate amount of 1% $H_2PtCl_6$ solution in 0.05 M $H_2SO_4$, diluted with an equal volume of methanol; this was then followed by heat treatment of the electrodes for 3 h at 200 °C in air. Electrodeposition of Pt, on the active side of Protech electrodes using the same $H_2PtCl_6$ (1%)–methanol solution (1:1 vol), was carried out at a constant current density of 2 mA $cm^{-2}$ to deposit ~0.05 mg $cm^{-2}$ of Pt; a gold foil was used as anode during electrolysis.

### *2.2. Assembly of single cells and performance evaluation*

The main components of a single cell assembly are as described in previous papers [5 - 7]. The essential components are two graphite plates, the M&E assembly and gaskets containing the gas inlet and outlet, and ribbed channels for the distribution of reactant gases behind the porous gas diffusion electrodes. The M&E assembly is positioned between two such graphite plates. The reference electrode (a small piece of fuel cell electrode) is embedded in the graphite plate on the anode side. Teflon-coated fiberglass cloth gaskets are placed between the membrane and each of the graphite current collectors to prevent gas leakage and to avoid excessive compression of the electrodes. Current collection from the fuel cell uses a copper plate positioned behind each of the graphite plates. Compression of the overall assembly is made by means of two 1/4 in. thick stainless steel end plates and four bolts. Teflon sheets are used for electric insulation of the single cell and the end plates. Though incorporation of a single cell in the test station with all its peripheral components (*e.g.*, temperature controller, humidification chamber, flow meters, back pressure regulator) has also been described in the referenced publications, the components of the single cell and the test station are illustrated in Figs. 2 and 3, respectively. The performance evalua-

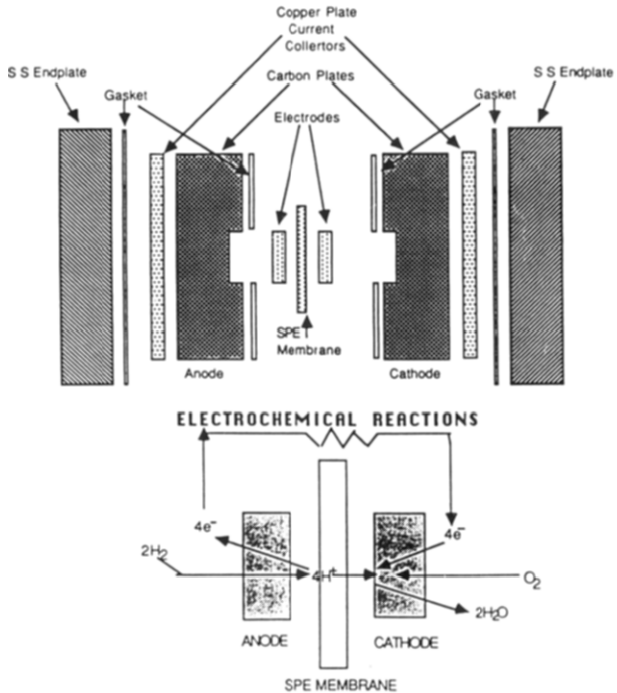


Fig. 2. Schematic of solid polymer electrolyte fuel cell assembly.

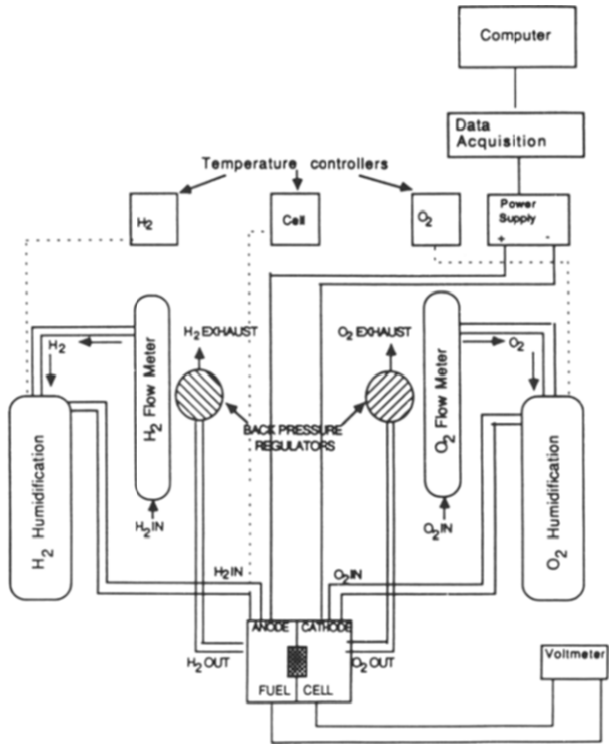


Fig. 3. Schematic of solid polymer electrolyte single cell test station.

tion was carried out using a microcomputer (IBM-XT), a power supply (HP 6033A), and a data acquisition unit (HP-3421A) interconnected through a GPIB bus. During performance evaluation, the fuel cell is connected in series with the power supply for its operation under galvanostatic load, and cell potentials, as well as half-cell potentials *versus* current density data, were recorded periodically. Measurements were made at different temperatures and pressures of reactant gases ($H_2$ at the anode and air/$O_2$ at the cathode).

## 3. Results and discussion

### *3.1. A comparison of the effects of sputter/deposition and wet chemical/electrochemical methods on the performance of single cells*

As stated in Section 1, one of the main objectives of this work was to find alternatives to sputter deposition to localize the platinum near the front surface of porous gas diffusion electrodes with low platinum loading electrodes. The cell potential–current density plots (Fig. 4) show that fuel cells with sputter deposited, and chloroplatinic acid treated, electrodes exhibit similar performances throughout the entire current density range (1 - 2000 mA $cm^{-2}$). This is not so in the case of the fuel cell with electrodes onto which a thin layer of Pt black was deposited. A close examination of the linear $E$ *versus* $i$ (Fig. 4), as well as of the semi-logarithmic ($E + iR$) *versus* $\log i$ (Fig. 5) plots shows that the oxygen electrode is only activation-

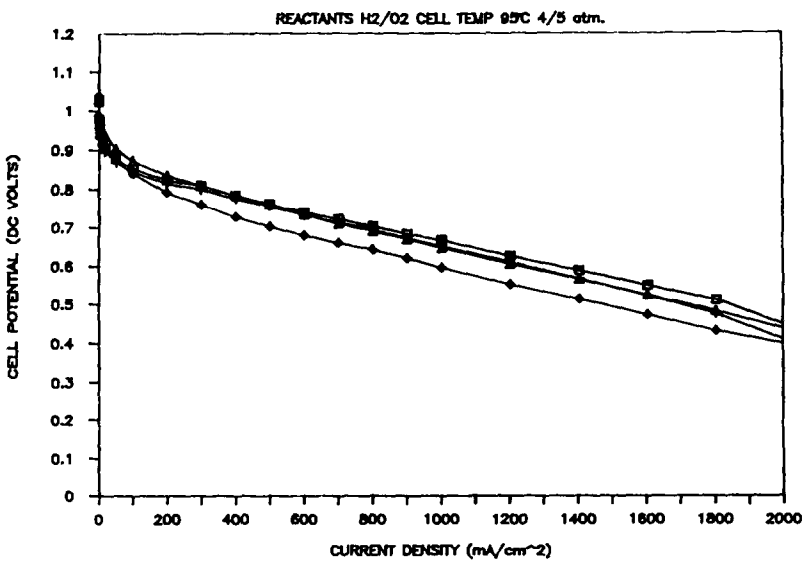


Fig. 4. Cell potential *vs.* current density plots for single cells with electrodes having localized Pt layer deposited by different methods, all operating at 95 °C and with $H_2/O_2$ at 4/5 atm. □, Sputter deposited; +, electrochemically deposited; △, chemically deposited from $H_2PtCl_6$; ◇, brushed with Nafion solution containing unsupported Pt. Pt loading on each electrode: 0.45 mg $cm^{-2}$.

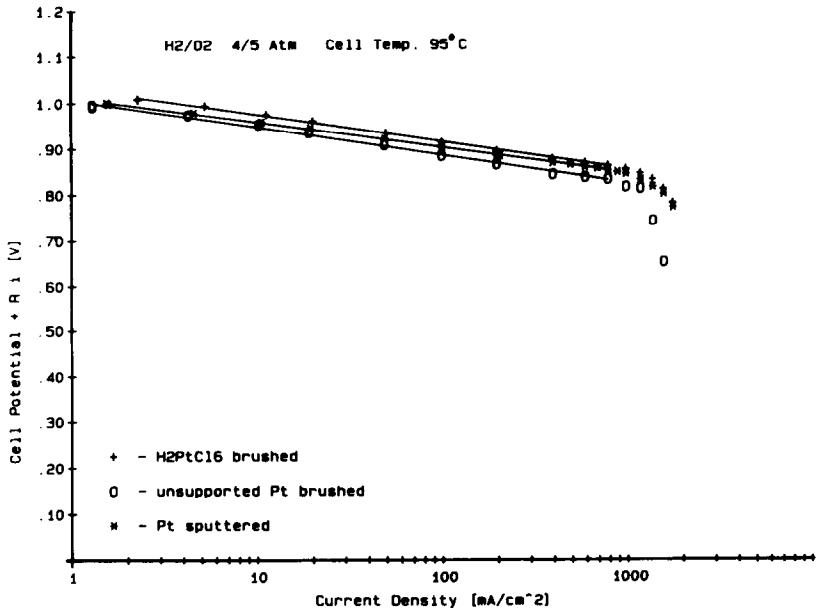


Fig. 5. Plots of $(E + iR)$ *vs.* log $i$ for single cells with electrodes having localized Pt layer deposited by different methods, all operating at 95 °C with $H_2/O_2$ at 4/5 atm. *, sputter-deposited; +, chemically deposited from $H_2PtCl_6$; ○, brushed with Nafion solution containing unsupported Pt. Pt loading on each electrode: 0.45 mg $cm^{-2}$.

controlled up to a current density of 1 A $cm^{-2}$. Figure 5 and Table 3 illustrate that the fuel cell with $H_2PtCl_6$-treated electrodes shows a higher oxygen electrode performance than the electrodes with the sputter deposited Pt and Pt/Nafion thin layers. This reflects a higher surface area of the $H_2PtCl_6$-treated electrode. The fuel cell with the Pt black-treated electrodes has an unusually high slope in the linear region of the $E$–$i$ plot and the departure from linearity occurs at a relatively low current density. The slopes of the linear regions of the $E$–$i$ plots in the other two cases are similar for identical operating conditions, but not low enough to reach the desired goals of power density (see Section 1.2). However, it is encouraging to note that the wet chemical method of chloroplatinic acid application, followed by the heat treatment, provides electrodes which exhibit similar performances to the sputter deposited electrodes.

### *3.2. Effects of membrane thickness on fuel cell performances*

Most of the LANL studies reported in refs. 5 - 7 used Nafion 117 membranes. Fuel cells with these membranes yield a slope of approximately 0.25 Ω $cm^2$ in the linear region of the $E$–$i$ plot. If the resistance of the test cell fixtures (0.05 Ω $cm^2$) is subtracted from this value, the slope of the $E$–$i$ plot (Table 3, linear region) will be reduced to 0.20 Ω $cm^2$. This value is still too high to reach current densities of 2 - 5 A $cm^{-2}$ at reasonable cell

TABLE 3

Effect of method of deposition of thin layer of platinum (0.05 mg $cm^{-2}$) on front surface of Prototech electrodes (20% Pt/C, 0.04 mg Pt $cm^{-2}$) on electrode kinetic parameters (see eqn. (1)) for $H_2/O_2$ solid polymer electrolyte fuel cell with 100 $\mu$m thick Nafion membrane

| Method of Pt deposition | Cell temperature (°C) | Pressure $H_2/O_2$ (atm) | Electrode kinetic parameters for cell | | | Current density at 0.9 V (mA $cm^{-2}$) |
|---|---|---|---|---|---|---|
| | | | $E_0$ (V) | $b$ (V) | $R$ ($\Omega$ $cm^{-2}$) | |
| Sputtered Pt | 50 | 1/1 | 0.930 | 0.044 | 0.339 | 7 |
| Sputtered Pt | 50 | 4/5 | 0.993 | 0.047 | 0.301 | 35 |
| Sputtered Pt | 70 | 4/5 | 0.983 | 0.040 | 0.252 | 46 |
| Sputtered Pt | 85 | 4/5 | 0.999 | 0.450 | 0.201 | 52 |
| Sputtered Pt | 95 | 4/5 | 0.997 | 0.500 | 0.189 | 61 |
| Unsupported Pt/Nafion, brushed | 50 | 1/1 | 0.964 | 0.052 | 0.501 | 12 |
| Unsupported Pt/Nafion, brushed | 50 | 4/5 | 0.956 | 0.048 | 0.452 | 48 |
| Unsupported Pt/Nafion, brushed | 70 | 1/1 | 1.024 | 0.059 | 0.505 | 10 |
| Unsupported Pt/Nafion, brushed | 70 | 4/5 | 1.014 | 0.052 | 0.462 | 51 |
| Unsupported Pt/Nafion, brushed | 85 | 4/5 | 1.008 | 0.045 | 0.414 | 61 |
| Unsupported Pt/Nafion, brushed | 95 | 4/5 | 1.005 | 0.044 | 0.368 | 35 |
| $H_2PtCl_6$ in $H_2O$–$CH_3OH$ — brushed | 50 | 1/1 | 0.978 | 0.056 | 0.338 | 19 |
| $H_2PtCl_6$ in $H_2O$–$CH_3OH$ — brushed | 50 | 4/5 | 1.024 | 0.053 | 0.341 | 72 |
| $H_2PtCl_6$ in $H_2O$–$CH_3OH$ — brushed | 85 | 4/5 | 1.019 | 0.044 | 0.253 | 80 |
| $H_2PtCl_6$ in $H_2O$–$CH_3OH$ — brushed | 95 | 4/5 | 1.020 | 0.056 | 0.189 | 83 |

potentials (>0.5 V). Thus, in this work, experiments were carried out with Nafion membranes having a thickness of 50 and 100 $\mu$m and the results of fuel cell performance were compared with those in fuel cells with the Nafion 117 membrane (thickness: 175 $\mu$m). The 100 $\mu$m membranes were of the "sweded type" (sweding was carried out to roughen the surfaces of the membrane and make it of uniform thickness). The performances of the fuel cells with the 50, 100 and 175 $\mu$m membranes are shown in Fig. 6. While the fuel cell with the Nafion 117 membrane begins to show mass transport limitations at a current density of 1 A $cm^{-2}$, this is not the case for the single cells with thinner Nafion membranes. The single cell with 100 $\mu$m membrane shows mass transport limitation at 1.8 A $cm^{-2}$ while the cell with 50 $\mu$m membrane shows no mass transport limitation up to the highest current

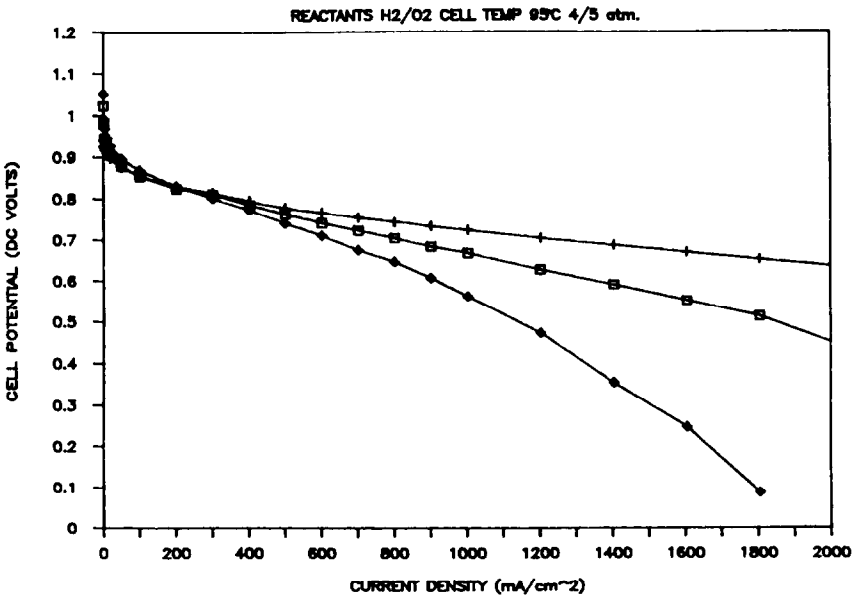


Fig. 6. Cell potential *vs.* current density plots for single cells with Nafion 117 membranes of two different thicknesses, operating at 95 °C with $H_2/O_2$ at 4/5 atm. Nafion, thickness: ◇, 175 μm; □, 100 μm; +, 50 μm. Pt loading on each electrode: 0.45 mg $cm^{-2}$.

density (2 A $cm^{-2}$) measurement. The electrode kinetic parameters extracted from these experimental results and using eqn. (1), are shown in Table 4. The agreement in the "pseudo *iR*" (all forms of overpotential which show a linear variation of potential with current density — mostly ohmic) corrected Tafel plots, Fig. 7, for oxygen reduction in the cells with the 100 and 175 μm thick membranes, are as expected. The sweded membrane (100 μm thick) shows a slightly higher resistance than expected on the basis of its thickness as compared with the thicker (175 μm) membrane (Table 4).

### *3.3. Dow membranes: the solution to attainment of super high power densities*

In the work to date, the highest power densities were obtained using Dow membranes as the electrolyte layer. A comparison of the performances of single cells using the Nafion and Dow membranes is illustrated in Fig. 8. The Nafion membranes had thicknesses of 175 and 100 μm while the Dow membranes were 125 μm thick. It is natural to expect a thinner membrane to have a lower resistance but, even if we take this into consideration, the Dow membrane has a lower specific resistivity (*i.e.*, higher specific conductivity) than Nafion. The reason for the higher specific conductivity of the Dow membrane than that of Nafion is that the monomer of the former may be represented by:

$$CF_2 = CFOCF_2CF_2SO_3H \qquad (6)$$

TABLE 4

Effect of thickness of Nafion membrane and of type of membrane on electrode kinetic parameters of $H_2/O_2$ solid polymer electrolyte fuel cell with Prototech electrodes (20% Pt/C, 0.40 mg Pt $cm^{-2}$) on to which a thin layer of Pt (0.05 mg $cm^{-2}$) was sputtered

| Membrane type and thickness | Cell temperature (°C) | Pressure $H_2/O_2$ (atm) | Electrode kinetic parameters for cell | | | Current density at 0.9 V (mA $cm^{-2}$) |
|---|---|---|---|---|---|---|
| | | | $E_0$ (V) | $b$ (V) | $R$ ($\Omega$ $cm^{-2}$) | |
| Nafion 117, 175 $\mu$m | 50 | 1/1 | 0.946 | 0.049 | 0.475 | 7 |
| Nafion 117, 175 $\mu$m | 50 | 3/4 | 1.003 | 0.048 | 0.428 | 50 |
| Nafion 117, 175 $\mu$m | 80 | 3/4 | 0.951 | 0.037 | 0.437 | 61 |
| Nafion 117, 175 $\mu$m | 85 | 3/4 | 1.007 | 0.046 | 0.298 | 70 |
| Sweded Nafion 117, 100 $\mu$m | 50 | 1/1 | 0.964 | 0.052 | 0.339 | 12 |
| Sweded Nafion 117, 100 $\mu$m | 50 | 4/5 | 0.956 | 0.048 | 0.301 | 48 |
| Sweded Nafion 117, 100 $\mu$m | 70 | 4/5 | 1.024 | 0.059 | 0.252 | 10 |
| Sweded Nafion 117, 100 $\mu$m | 85 | 4/5 | 1.008 | 0.045 | 0.201 | 61 |
| Sweded Nafion 117, 100 $\mu$m | 95 | 4/5 | 1.005 | 0.044 | 0.189 | 35 |
| Nafion 117, 50 $\mu$m | 50 | 1/1 | 0.833 | 0.061 | 0.188 | $<1$ |
| Dow membranes | 50 | 1/1 | 0.955 | 0.061 | 0.195 | 7 |
| Dow membranes | 50 | 4/5 | 0.995 | 0.053 | 0.157 | 42 |
| Dow membranes | 70 | 1/1 | 0.912 | 0.062 | 0.153 | 1.6 |
| Dow membranes | 70 | 4/5 | 0.994 | 0.053 | 0.116 | 43 |
| Dow membranes | 85 | 4/5 | 1.002 | 0.053 | 0.111 | 62 |
| Dow membranes | 95 | 4/5 | 1.000 | 0.549 | 0.110 | 54 |

while that of the later is:

$$CF_2 = CFOCF_2\underset{\displaystyle CF_3}{\underset{|}{C}}FOCF_2CF_2SO_3H \qquad (7)$$

Hence, there is a greater number of sulfonic acid groups in the Dow polymer membrane than in the Nafion polymer membrane. Expressed differently, the Dow proton conducting polymer has a lower equivalent weight than Nafion.

Figure 8 shows that the cell potential–current density plots overlap in the low current density region (say up to 50 mV). This means that the activation-controlled behavior is unaffected by the characteristics of the membrane (Dow *versus* Nafion, Nafion thick *versus* thin). One can easily

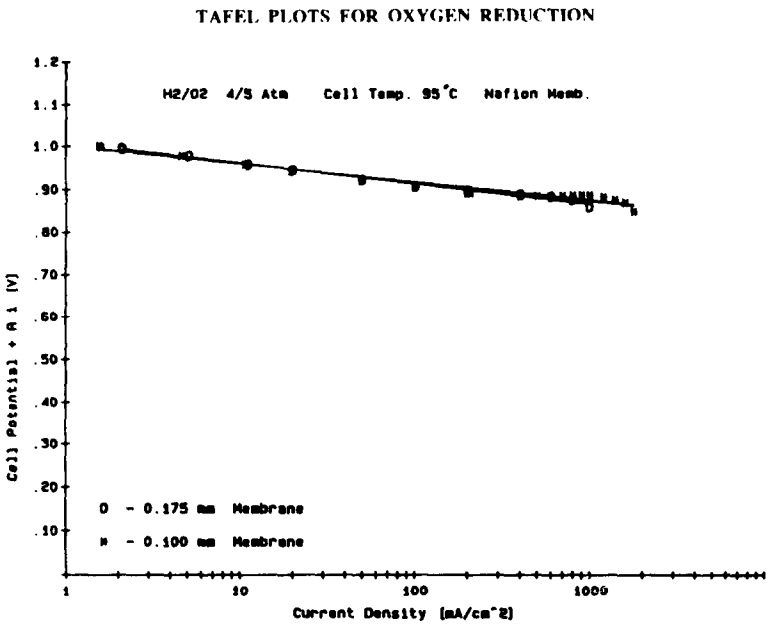


Fig. 7. Plots of $(E + iR)$ *vs.* log $i$ for single cells with Nafion membranes of two different thicknesses, operating at 95 °C with $H_2/O_2$ at 4/5 atm. Nafion 117, thickness: ○, 175 μm; *, 100 μm. Pt loading on each electrode: 0.45 mg $cm^{-2}$.

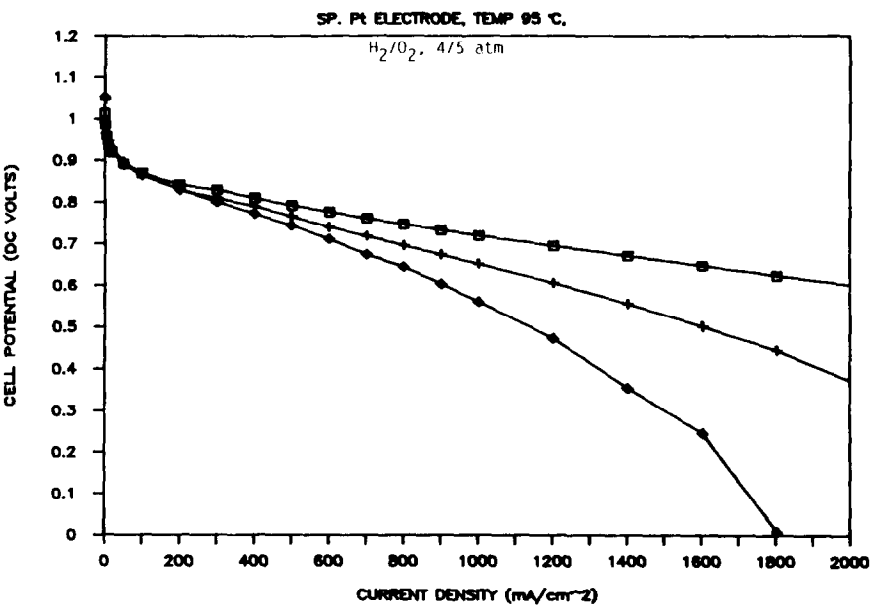


Fig. 8. Cell potential *vs.* current density plots for single cells with different membrane materials, operating at 95 °C with $H_2/O_2$ at 4/5 atm. □, Dow membrane, 125 μm; ◇, Nafion 117, 175 μm; +, Nafion 117 (sweded), 100 μm. Pt loading on each electrode: 0.45 mg $cm^{-2}$.

interpret this result on the basis that the electrochemical reaction occurs, to a large extent, within the pores and the surface of the electrodes which are coated with the proton-conducting membranes. With increasing current density, the role of the membrane (type, thickness) is dominant and consequently the linear region slopes are different. One significant result is that that linear region slope in the cell with the Dow membrane (thickness 175 $\mu$m) is less than that in the cell with the Nafion membrane (thickness 100 $\mu$m), even though the thickness of the Dow membrane is greater than that of the Nafion membrane. This result can be explained by the fact that the Dow membrane has a higher specific conductivity than that of the Nafion membrane.

There is a second interesting observation in the $E$–$i$ plots. The departure of the $E$–$i$ plot from linearity at the higher current density appears to depend on the thickness of the membrane (*cf.* the results of Nafion membranes 175 and 100 $\mu$m thick) and the type (*cf.* Dow membrane 125 $\mu$m with Nafion 100 $\mu$m). Departures from linearity at the high current densities are associated with mass-transport-controlled processes. Generally, these are due to mass transport limitations of reactants reaching the active sites in the electrode or of products (or inert gases such as $N_2$ when air instead of oxygen is used) moving away from the electrocatalytic sites. However, the electrode structures and conditions of humidification of reactant gases were identical in the three cases. It is very likely that transport processes within the membrane can be rate-limiting. The transporting species are protons, which migrate from the anode to the cathode under the influence of the electric field, and water molecules which are carried with the protons. It is estimated that 3 - 6 water molecules are transported with the protons. Due to the resulting concentration gradient of water molecules in the cell during operation, one can expect water molecules to diffuse from the cathode to the anode. Mass transport limitations could occur due to any one, or more of these processes. The Dow membrane shows a linear behavior up to a current density of 2 A $cm^{-2}$. This is not the case in the cell with the Nafion membrane which is slightly thicker than the Dow membrane. This result provides insight to different types of proton conduction (say, Grotthus type in a Dow membrane *versus* classical proton transport through the electrolyte in Nafion). It is interesting to note that in previous studies it was observed that when mass transport limitation begins on one electrode, it also sets in on the other at the same current density. A detailed modeling analysis of the mass transport processes is necessary to interpret the result in the higher current density range.

The electrode kinetic parameters for the cells were calculated as described briefly in Section 1.2. The parameters $E_0$ and $b$ are unaffected by the membrane. However, $R$, which represents the rate of increase of cell potential in a linear manner with the current density, depends on the membrane type and its thickness. The most significant contribution to $R$ is the ionic resistance of the membrane, as has been shown previously using high frequency measurements [7]. The striking result is that $R$ is a factor of

two less for the cell with the Dow membrane (thickness 125 μm) than for the one with the Nafion membrane. This result follows from the fact that the Dow membrane has a lower specific resistance. The calculated value of $R$ is always slightly less than the slope of the linear region in the $E$ *versus* $i$ plot. For example, for the cell with the Dow membrane operating at 95 °C, the $R$ is 0.110 while the slope of the linear region is 0.113. The reason for this is that the apparently linear slope of the $E$–$i$ plot includes a small contribution of the charge transfer resistance of the oxygen reduction reaction. In the cells used in this work the test cell fixtures have a resistance of 0.05 ohm $cm^2$. If this is excluded from the values of $R$ and of the slope of the $E$–$i$ line, the resulting values are only 0.06 and 0.08 Ω $cm^2$, respectively. The latter value is the same as that of the slope of the $E$–$i$ plot in the best Ballard cells. Using the calculated values of $R$, the ($E$ + $Ri$) *versus* log $i$ plots (Fig. 9) were constructed for the cells with the Dow (125 μm) and Nafion (100 μm) membranes operating at 95 °C and 4/5 atm. The Tafel behavior is observed for the former cell over the entire current density range whereas, for the latter, there is departure from the Tafel line at the same current density as that in the $E$–$i$ plot where it departs from linearity.

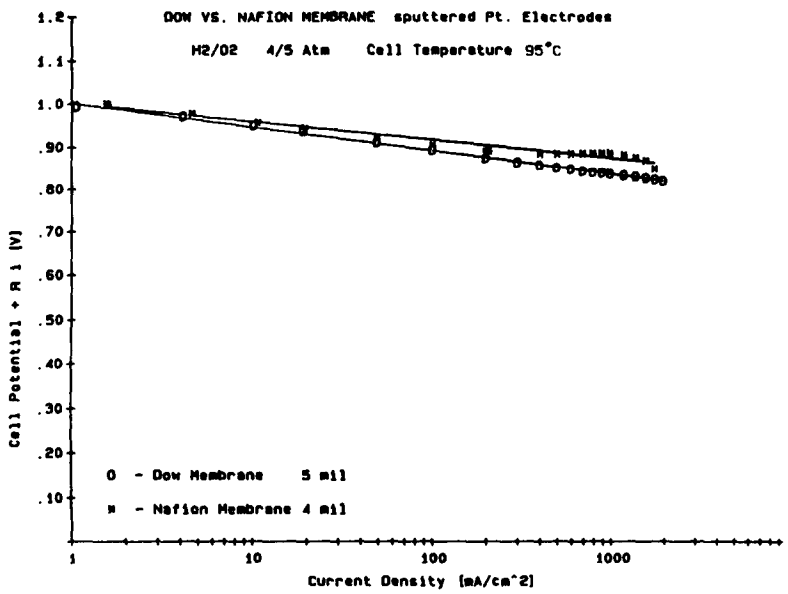


Fig. 9. Plots of ($E$ + $iR$) *vs.* log $i$ for single cells with different membrane materials, operating at 95 °C with $H_2/O_2$ at 4/5 atm. ○, Dow membrane, 125 μm; *, Nafion 117, 175 μm. Pt loading on each electrode: 0.45 mg $cm^{-2}$.

Another result is worth mentioning. The half and single cell potentials are plotted as a function of current density (Fig. 10) for the cell with the Dow membrane. The hydrogen electrode exhibits a linear behavior throughout the entire current density range. The hydrogen overpotential at 2 A

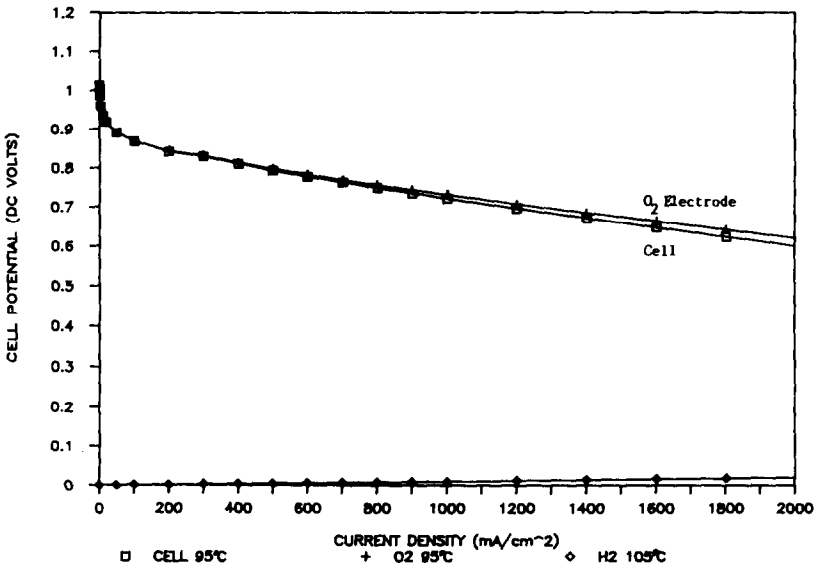


Fig. 10. Cell and half cell potentials *vs.* current density plots for a single cell with Dow membrane (thickness: 125 $\mu$m) and Pt-sputtered Prototech electrodes (Pt loading: 0.45 mg $cm^{-2}$) operating at 95 °C with $H_2/O_2$ at 4/5 atm.

$cm^{-2}$ is only 20 mV. Thus the charge transfer resistance due to the hydrogen electrode is only 0.01 $\Omega$ $cm^2$ which is the contribution of this electrode to the calculated $R$ value or the measured slope of the cell potential *versus* current density plot.

## 4. Conclusions

The conclusions which may be drawn from these studies are:

(i) The chloroplatinic acid method of treatment of the electrodes provides a satisfactory alternative, and considerably more economic, method to sputtering for the deposition of a thin layer of Pt on the front surfaces of the electrodes, essential for the attainment of high power densities.

(ii) Use of thinner membranes is advantageous from the points of view of lowering the ionic resistance and lowering mass transport limitations at higher current densities.

(iii) Striking results have been obtained in cells with the Dow membrane having a higher ionic conductivity, less mass transport limitations ($H^+$ and $H_2O$), and better water management characteristics than Nafion.

(iv) The performances of solid polymer electrolyte fuel cells with low platinum loading electrodes are approaching those with ten times the platinum loading with regard to attainment of high power densities.

## Acknowledgements

This work was supported by a contract from DARPA/ONR, Code 1113 ES. The authors are grateful to Dow Chemical (via Drs Glenn Eisman and Jeffrey Gunshor), Freeport, Texas, for providing the Dow polymer membranes used in this work.

## References

1 (a) J. K. Stedman, Abstr., *1985 Fuel Cell Seminar*, Courtesy Associates, Washington, DC, 1985, p. 138; (b) R. Warnock, Wright-Patterson Air Force Base, personal communication.
2 (a) D. Watkins, D. Kircks, D. Epp and A. Harkness, *Proc. 32nd Annu. Power Sources Conf., Cherry Hill, NJ, June 9 - 12, 1986*, The Electrochemical Society, Inc., 1986, p. 590; (b) D. Watkins, Ballard Technologies, Inc., personal communication, 1987.
3 O. J. Adlhart and M. J. Rosso, Ergenic Power Systems, Inc., Wyckoff, NJ, personal communication.
4 K. Strasser, Siemens, Erlangen, F.R.G., personal communication.
5 S. Srinivasan, E. A. Ticianelli, C. R. Derouin and A. Redondo, *J. Power Sources, 22* (1988) 359.
6 E. Ticianelli, C. R. Derouin, A. Redondo and S. Srinivasan, *J. Electrochem. Soc., 135* (1988) 2209.
7 E. A. Ticianelli, C. R. Derouin and S. Srinivasan, *J. Electroanal. Chem., 251* (1988) 275 - 295.
8 J. O'M. Bockris and S. Srinivasan, *Fuel Cells: Their Electrochemistry*, McGraw-Hill, New York, 1969.
9 A. J. Appleby and F. R. Fowkes, *Fuel Cell Handbook*, Van Nostrand Reinhold, New York, 1988.
10 S. Srinivasan, *J. Electrochem. Soc., 136* (1989) 41C.
11 M. A. Enayatullah and J. O'M. Bockris, in S. Srinivasan, S. Wagner and H. Wroblowa (eds.), *Proc. Symp. on Electrode Materials and Processes for Energy Conversion and Storage, Proc. Vol. 87-12*, The Electrochemical Society, Pennington, NJ, 1987, p. 256.